Egypt. J. Chem. **Vol. 66** No. 11 pp. 327 -344 (2023)

Egyptian Journal of Chemistry

http://ejchem.journals.ekb.eg/

A Novel Dual Layered Hydrophobic/Hydrophilic Composite Tri-bore Hollow Fibre Membrane for Vacuum Membrane Distillation-Preparation and Evaluation

Eman Farag[1*], Reem Ettouney[2], Elham El-Zanati[1], Mahmoud El-Rifai[2]

[1]Chemical Engineering and Pilot Plant Department, Engineering Research Division, National Research Centre, Dokki, Giza, Egypt.

[2]Chemical Engineering Department, Faculty of Engineering, Cairo University, Giza, Egypt.

Abstract

Polyvinylidene fluoride (PVDF) was used to create microporous, hydrophobic/hydrophilic dual-layer, tri-bore hollow fiber membranes under various operating conditions and with various polymeric dope compositions. Nanoparticles of silicon dioxide and titanium dioxide were added to both the outer and interior layers. To produce fibers with various morphologies, the concentration of SiO_2 nano powder in the inner dope solution was changed. The created membranes were examined under a microscope to determine their shape, level of roughness (AFM), contact angle, and mechanical characteristics. The produced membrane's suitability for vacuum membrane distillation (VMD) is assessed. This study aims to relate the polymeric dope composition and spinning conditions to the preparation parameters, namely the hydrophobic/hydrophilic tri-bore hollow fiber membrane flux.

Keywords: triple orifice**,** hydrophobic/hydrophilic dual-layer membrane, multi-bore hollow fibers, membrane distillation, nanoparticles**.**

Introduction

To solve the global water shortage, a number of solutions have been suggested, including desalination and wastewater recycling [1]. Membrane distillation (MD), a new and promising technique, has been given a lot of thought when it comes to alternatives for desalinating water. A microporous hydrophobic membrane is used in vacuum membrane distillation (VMD) as a barrier to prevent contact between the aqueous feed stream and the produced water vapor [2-4]. Higher permeation flux, improved thermal efficiency, and the ability to use sustainable energy sources including geothermal resources, solar energy, and waste heat streams make VMD superior to previous MD designs [5-7].

The membrane is an important component of the desalination process in MD setups. To avoid being wet by the feed solution, the optimal MD membrane ought to be hydrophobic. It should have good mechanical qualities, a high penetration flux, and excellent salt rejection. [8,9]. Due to its high operability and tunable membrane forming qualities, polyvinylidene fluoride (PVDF) is used extensively. PVDF membranes for VMD should be rationally designed with high mechanical strength, adequate stability for frequent usage, and long-term preservation in consideration [10-13]. For VMD applications, numerous PVDF hollow fiber membranes have been created. The increase in permeation flux is favored by large porosity and thin walls, however this compromises the mechanical strength of the resulting membranes. [14-23].

In an effort to modify the membrane structure and enhance its qualities, appropriate additives are added to the PVDF dope solution as part of efforts to improve the mechanical properties of PVDF

*Corresponding author e-mail: demfarg@gmail.com

Receive Date: 11 August 2022, Revise Date: 03 September 2022, Accept Date: 05 September 2022

DOI: 10.21608/EJCHEM.2022.153982.6720

membranes. To strengthen the structure of PVDF membranes, mixed matrix membranes including nanoparticles were created [24-29]. Hydrophilic/hydrophobic dual-layer membranes for VMD have been observed to increase the permeate water flux while retaining high salt rejection and membrane high mechanical strength [30-36]. It has also been suggested that using multi-bore hollow fibers (MBHF) will increase the membrane's mechanical stiffness [37-44]. In these attempts, PVDF was frequently employed as the structural matrix support [45-48]. Thus, the intrinsic properties of PVDF continued to govern the total mechanical strength of the membrane. A better option for creating MD membranes with synergistic features would be if the mechanical strength of PVDF could be increased by the addition of various hydrophilic substrates to create a composite multi bore hollow fiber membrane.

The two primary methods for producing hydrophilic/hydrophobic dual-layer (H/H DL) composite hollow fiber membranes for VMD are co-extruding and surface coating modification. Through the use of a co-extrusion method, a triple-nozzle spinning technology has been created for the one-step preparation of composite dual-layer hollow-fiber membranes. [49-50].

To far, no (H/H DL) composite multi bore hollow fibers (MBHFC) have been co-spun employing a triple orifice spinneret from two compatible dope solutions for MD applications. While silicon dioxide nanoparticles (SiNPs) were chosen as an additive to the PVDF inner layer due to their good elastic properties, slight hydrophilicity, and moderate compatibility with PVDF, fluorinated titanium dioxide nanoparticles (FTiNPs) were used to create a highly hydrophobic PVDF outer layer. To improve its mechanical stretchability, the inner layer was treated with a non-toxic solvent called tri ethyl citrate (TEC).
To design and optimise each layer with a particular purpose, a thorough examination of the spinning principles of composite tri-bore hollow fibres (TbHFC), three-needle triple orifice spinneret is done. The characteristics of the hydrophilic-hydrophobic tri-bore hollow fibre membranes (H/H-TBF) made from composite PVDF were then identified. In order to be effective for VMD applications, the resulting TbHFC membrane must concurrently exhibit acceptable wetting resistance, permeation flux, salt rejection, and mechanical stability.

1. Experimental

2.1 Materials

PVDF powder, 1H, 1H, 2H, 2H-perfluorooctyltriethoxysilane, and fluorinated alkyl silane (FAS) used for the functionalization of TiO_2 were acquired from Alfa Aesar. 1-Methyl -2-pyrrolidinone (NMP), Titanium dioxide (TiO_2) powder (particle size: 20 nm), silicon dioxide nano powder (SiNPs) (10-20 nm particle size) and Tri ethyl citrate (TEC) were purchased from Sigma Aldrich. Lithium Chloride (LiCl) (anhydrous 99%, MW= 42.39 g/mol) was obtained from Alpha Chemica. Absolute ethanol, propan-2-ol and glycerol were acquired from Fisher.

2.2 Synthesis of fluorinated TiO_2 nanoparticles as a hydrophobic enhancer

The contact angle (CA) of a water droplet on a solid surface, which is influenced by both the surface's geometric microstructure and chemical makeup, is typically used to measure wettability. The intrinsic CA of PVDF is roughly 86°.TiO_2 nanoparticles have a high surface energy and are hydrophilic due to the many hydroxyl groups on their surface. They also have a tendency to form irregular aggregates. FAS molecules are easily altered on the surface of hydroxyl rich films despite the fact that they are hydrophobic and have a contact angle of 109° on a flat surface. Due to the existence of C-F and C-H groups, TiO_2 nanoparticles were efficiently treated with FAS in the current work to minimize their surface-free energy. TiO_2nanoparticle dispersion in organic solvents is enhanced by FAS, which also reduces nanoparticle agglomeration and increases the membrane's hydrophobic characteristics. [51-53].

Using a hydrothermal reaction technique, 30 g of TiO_2 particles were combined with 100 ml of ethanol that included 1 ml of FAS to create the modified TiO_2 particles. The hydrophobic modified-TiO_2 particles (FTiNPs) were formed after repeated washing with ethanol and drying at 120°C for 2 hours while the mixture was aggressively agitated at 50 ^{o} for 2 hours at 600 rpm. These TiO_2 particles are known as FTiNPs because FAS molecules have partially replaced the hydroxyl groups on the particle surface [51].

2.3 Characterization of the fluorinated TiO_2 particles

A Fourier-transform infrared (FT-IR) spectroscope was used to analyze the phases of untreated and treated TiO_2 particles (Burker vertex 70). By pressing

the sample with KBr on a pellet and using scans with a signal averaging 4000-400 cm-1 scans at a resolution of 4 cm-1, each spectrum was acquired in transfer mode. Infrared (IR) cards were used to produce transparent films.

2.4 H/H-TBF dopes preparation

To prepare the outer layer spinning dope, the predetermined amount of FTNPs was added to the organic solvent NMP and the solution was ultrasonicated for 30 min at 55 °C to prevent nanoparticles' agglomeration. PVDF and LiCl (pore-forming additive) were added gradually into the prepared solution of NMP and FTNPs. The mixed solution was mechanically stirred at 400 rpm for 6 h at 55 °C to form a homogeneous solution. After 6 h of continuous stirring, a clear four-component solution was obtained.

To prepare the inner layer dope solution with perfect adhesion and stability with the outer dope solution of TbHFC membranes, three dope solutions are prepared with different compositions of SiNPs. The concentrations of PVDF, LiCl, TEC and NMP are kept constant for all blends while only the SiNPs content was changed. SiNPs were added into the organic solvent NMP in various mass ratios and the solution was ultrasonicated for 30 min at 55 °C to prevent nanoparticles agglomeration. PVDF, TEC and LiCl (pore-forming additive) were added gradually into the prepared solution of NMP and SiNPs. The mixed solution was mechanically stirred at 400 rpm for 6 h at 55 °C to obtain a homogeneous solution. The solutions were stored in containers at room temperature and degassed for 12 h before being transferred to the spinning step. Hollow fibers were spun by the dry/wet technique described in section (2.6). The dope compositions for the three inner dopes and the outer dope are summarized in Table 1.

Table 1: Compositions of dopes and coagulants used in the preparation of the dual-layer hollow fiber membranes.

	Outer layer composition (wt. %)				Inner layer composition (wt. %)					Bore fluid composition (wt. %)	External coagulant (v. %)	
TBF	PVDF	NMP	LiCl	FTiNPs*	PVDF	NMP	LiCL	TEC	SiNPs[a]		First	second
H/H1									0.1	Water:80 NMP: 20	Water : 100	Water:97.8 IPA:2 Glycerol:0.2
H/H2	17	82	1	0.5	15	82	1	2	0.2			
H/H3									0.4			

* Concentration of FTNPs was based on total weight of the mixed solution.
[a] Concentration of SiNPs was based on total weight of the mixed solution.

2.5 Preparation of flat-sheet membranes

The H/H$_2$-TBF membrane outer and inner layers were created as the top and support layers of the modified PVDF dual-layered flat sheet membrane (MT), respectively. For comparison, a tidy PVDF membrane (M0) comprised of 17 percent PVDF, 82 percent NMP, and 1 percent LiCl was created. A 400 m-gap casting knife was used to cast a dope onto a glass plate. To mimic the phase inversion process that would occur when NMP/water solution was employed as the bore fluid, the glass plate was immediately submerged into an NMP/water bath. Following their removal from the glass plate in the water bath, the developing flat-sheet membranes were transferred to a treatment bath containing water, IPA, and glycerol with corresponding compositions of 97.8, 2, and 0.2 v percent for 2 days to remove the remaining solvent. For subsequent measurements, the flat-sheet membranes were dried.

2.6 Spinneret and block design

Triple orifice spinnerets -three passages: one for inner bore fluid, one for the first polymer layer (inner surface), and the third for the second polymer layer (outer surface)) and their block- were designed by E. El Zanati, and locally manufactured at Hassco. The spinnerets have three bores as shown in Figure 1. Unlike the conventional single-bore spinneret, the 3-bore H/H TBF spinneret has three needles, uniformly distributed within the spinneret space. The spinning block shown in Figure 2 was designed to hold the spinnerets. It has three input ports for the bore fluid, polymer 1, and polymer 2 respectively, and a passage for the heating fluid, to keep the polymers inside the block in the liquid state. The following sections present the measures undertaken to investigate and optimize the spinning process and the operating parameters which would affect the TbHFC membrane preparation.

2.7 H/H-TBF Spinning

A typical hollow fiber spinning process with liquid bore (NMP/water), a coagulation bath, and the

treatment bath are shown in Figure 3. During spinning, the two diluted polymer solutions are co-extruded with an inert bore fluid at specified flow rates through the spinneret by three precise peristaltic pumps (BT100-2J). The bore fluid is extruded at room temperature, whilst hot water (~ 45ºC) enters the heating circuit of the block. As the nascent membrane passes through a certain air gap, a small amount of its solvent is evaporated before entering the liquid nonsolvent (water) coagulating bath by free fall. The fiber undergoes rapid coagulation/cooling in the liquid bath causing the solidification of the polymer-rich region and forming the membrane. Figure 4 depicts the bench scale spinning system (a) and its front view (b).

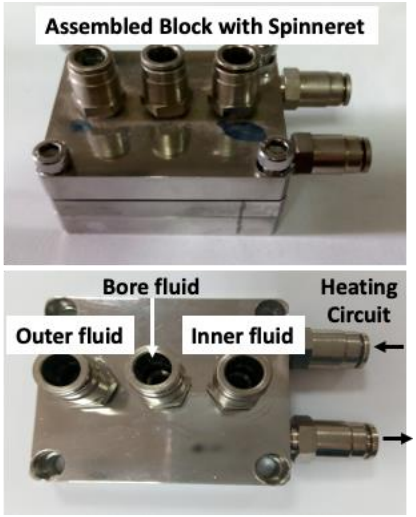

Figure 2: Assembled and detailed spinneret block

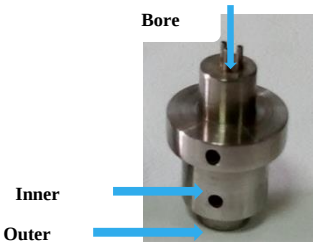

Figure 1: Spinnerets of Three with Triple Orifices

The parametric study is conducted on the preparation conditions of the composite H/H-TBF membranes. The influencing parameters are the flow rates of the two dope solutions, the flow rate of bore fluid, and the air gap distance from the block end to the water surface interface at the coagulation bath. The results of the optimum blends of inner and outer layers compositions were used in the parametric study for the spinning conditions. The details of the spinning conditions are summarized in Table 2. To effectively control phase inversion during membrane formation and to obtain the desirable membrane structure and morphology, the solidified fiber was immersed in a second bath for the treatment process. The nascent fibers were immersed in a treatment bath containing water/IPA/glycerol with composition 97.8, 2 and 0.2 v% respectively for 3–5 days to remove the residual solvent and non-solvent. Finally, they were cut into 15 cm long pieces and dried under ambient conditions.

Table 2: Parameters of the different spinning conditions

	TBF1	TBF2	TBF3	TBF4	TBF5	TBF6	TBF7	TBF8	TBF 9	TBF 10
Outer dope flow rate (ml/s)	1.6									
Inner dope flow rate (ml/s)	0.63			0.29	0.63	0.95	1.3	1.6	0.95	
Bore fluid flow rate (ml/s)	0.29	0.42	0.55	0.29						
Air gap (cm)	3								0	6
Take up rate (cm/min)	Free fall									

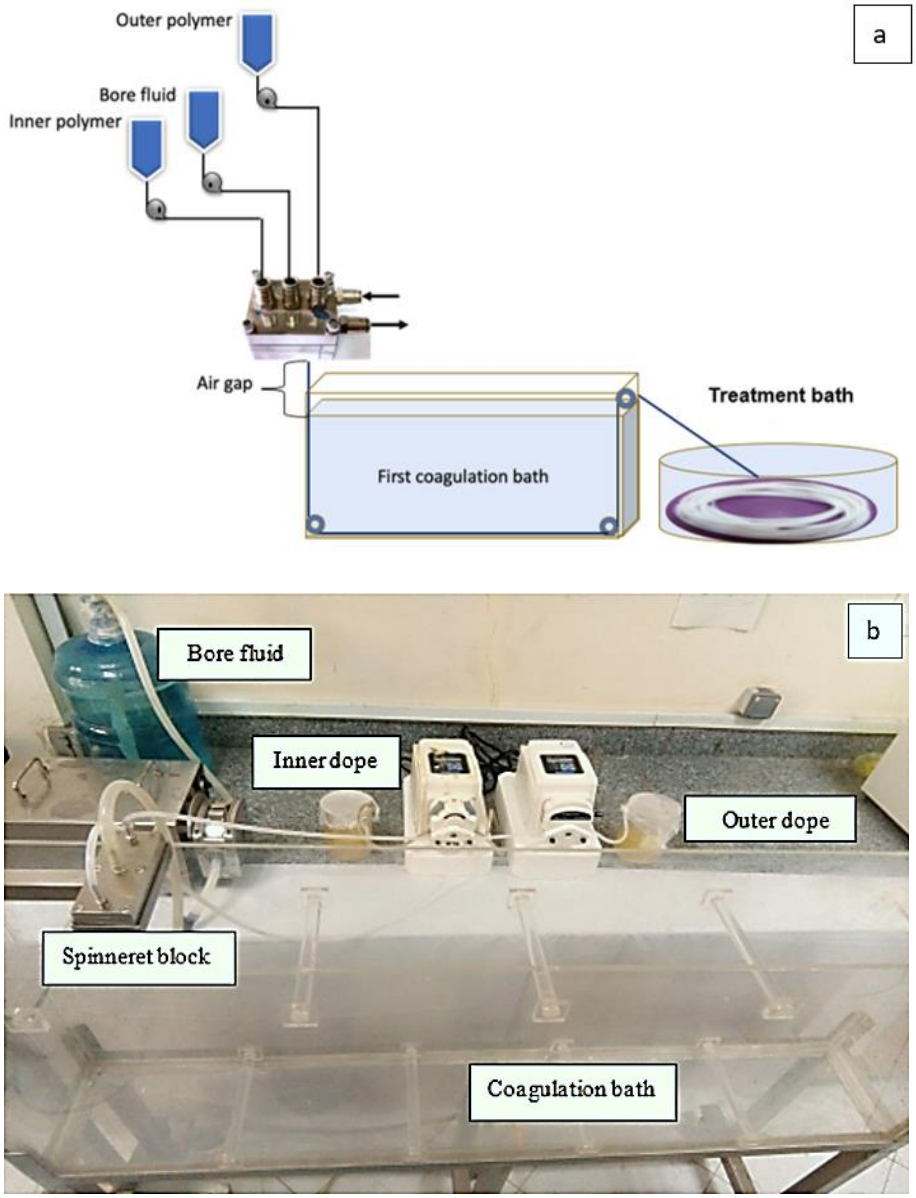

Figure 3: Lab scale spinning system set-up a) flow diagram and b) frontal view

2.8 Module fabrication

The membrane module was specifically designed and fabricated in the National Research Center laboratory. Five hydrophobic/hydrophilic hollow fibers were coaxially packed into an acrylic housing. A five-holed cover was welded to each end of the acrylic housing. Each hollow fiber was introduced through the corresponding hole of the top and bottom covers and then it was fixed with epoxy resin at both ends as shown in figure (4. a). The five-holed covers were designed to maintain the hollow fibers parallel inside the tubular module, keeping a constant space between them and between the fibers and the tubing surface. The effective length of the VMD tubular module was 10 cm. Both sides of the assembled module were covered with end caps with ports to facilitate the process of connecting hoses as shown in figure (4.b).

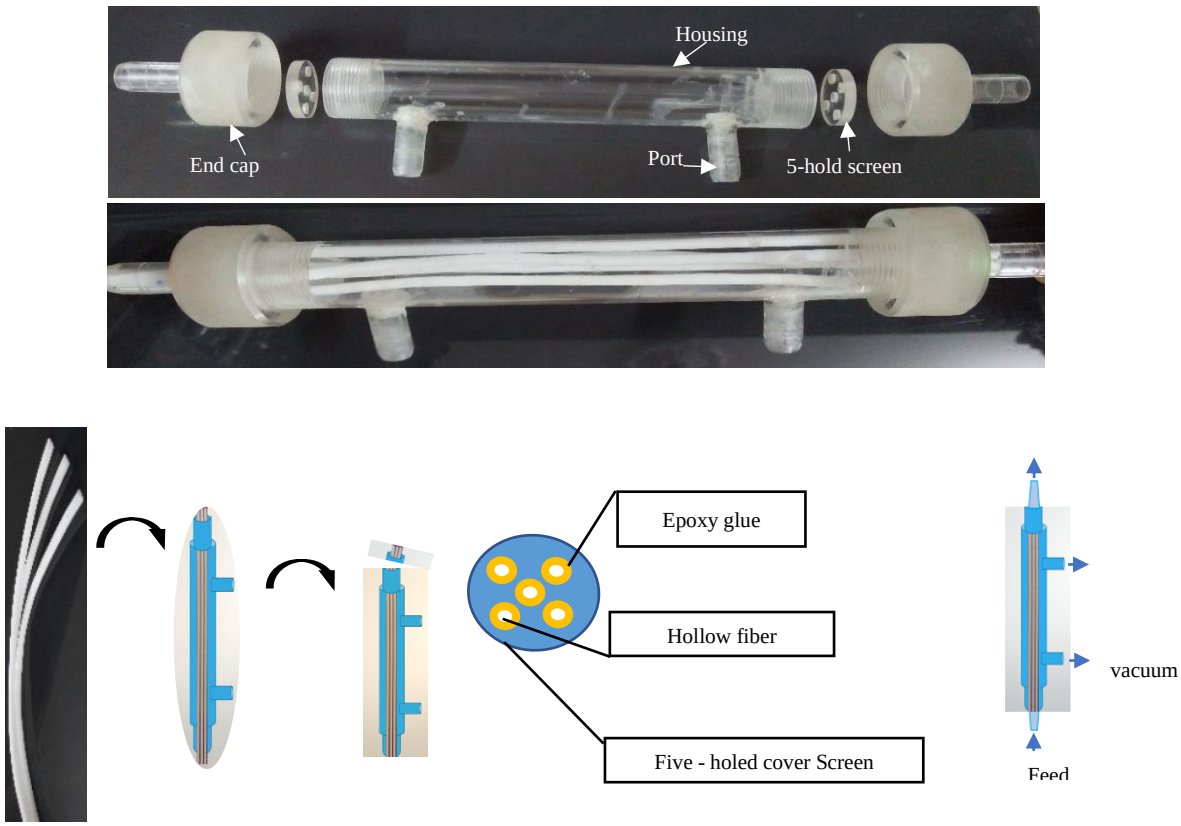

Figure 4: a) final shape of hollow fiber module, b) fibers packing steps in to acrylic tube

2.9 Membrane Characterization

Scanning electronic microscopy (SEM)

SEM was used to characterize the membrane morphology and surface topography. The dry samples were covered with a gold sputtering to provide for electrical conductivity. Images were taken on a JEOL 5410 scanning electron microscope (SEM), operating at 10 kV.

Atomic force microscope (AFM)

The topography of the prepared membranes was monitored via the AFM, Flexaxiom Nanosurf, and C3000 at the dynamic mode (non-contact) to confirm hydrophobic modification and to detect the changes to the membrane surface. The AFM measurements were conducted at room temperature using an NCLR rectangular -shaped silicon cantilever with a resonance frequency of 9 kHz.

Contact angle

The contact angles of the prepared PVDF membranes were determined by (SCA 20, OCA 15EC) using the sessile drop method (Preparation and finishing of cellulosic fibers, Textile research Division, NRC). The volume and contact time were 10µl and 10s respectively. This was carried out five times for each of the membranes.

Mechanical properties

The mechanical properties for hollow fiber membranes were determined with an Instron Tensiometer (Model 5542) from Instron Corp. at room temperature. The fiber was clamped at both ends with an initial length of 50 mm. A constant elongation rate of 50 mm/min was fixed for all measurements. For each spinning condition, the average value obtained from at least three samples was reported.

2.10 VMD desalination experiments

The VMD experiments were carried out to evaluate the permeation flux and salt rejection percentage (SR%) of the 3- bore hollow fiber membranes under optimized operating conditions. After ensuring that the membrane module was water tight, the VMD experiments were carried out. Figure 5 illustrates the lab-scale VMD unit using the prepared H/H TbHF membrane module. The feed saline solution temperature and flow rate were adjusted at 65°C and 0.62 l/min, respectively, while an approximately -1 bar pressure (zero absolute pressure) was applied to induce the evaporation of the solution through the membrane. The heated feed is introduced on the lumen side of the fibers through a peristaltic pump. Vacuum is applied on the outer side (module shell side) through a vacuum pump. The generated vapor is transferred through the membrane and is directed to the condenser. All experiments were carried out for 30 min. The flux was calculated using equation (1):

$$J_W = V/A \quad (1)$$

Where:

J_W is the volumetric membrane flux; l/m^2.h, V is the volumetric flow rate of the permeate; l/h and A is the effective membrane area; m^2. The salt rejection (SR) is calculated from equation (2):

$$SR = (1 - C_P/C_F) * 100 \quad (2)$$

Where:

C_P is the final salt concentration of the permeate stream and C_F is the initial salt concentration of the feed.

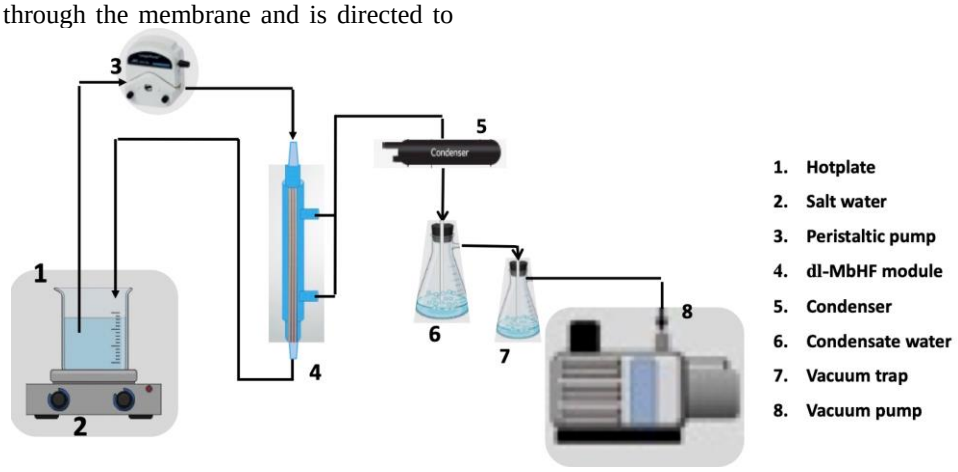

Figure 5: Process diagram of the lab scale VMD unit

3. Results and discussion

3.1 Fourier Transform Infrared Spectrophotometer (FTIR)

To ensure non-wetting of the membrane in VMD operation, the ideal material for MD membranes is required to possess low free surface energy. Polytetrafluoroethylene (PTFE) with a low free surface energy of 18.5 mN/m and polyethylene (PE) of 20–25 mN/m free surface energy are better than PVDF which has a surface energy of 30.3 mN/m [54]. However, polyethylene has a low melting point, while PTFE is difficult to process. PVDF is more processable as it can be dissolved in common organic solvents and hence, membrane fabrication by the non-solvent induced phase inversion process is possible. To lower the surface energy, self-synthesized FTiNPs were incorporated into the outer layer of the dual-layer PVDF hollow fiber membrane. Figures 6. a and 6. b show the FTIR spectra of the unmodified TiO_2 and Fluorinated TiO_2 nano particles as a hydrophobic enhancer. The band at 950.17cm^{-1} is attributed to the asymmetric stretching vibration of the Si–O–Ti species as shown in Figure (7. b), which proves the dehydration reaction of hydrolytic FAS molecules and TiO_2 particles [53].

Compared to the spectrum of unmodified TiO_2 in Figure (6. a), the FTiNPs have three peaks at 1144, 1210, and 1240.27 cm^{-1}, which are attributed to the stretching vibration of –CF2– and –CF3 groups, indicating that the fluorine containing FAS has been successfully synthesized. Figure 7 is a photograph of a spherulitic water droplet on the FTiNPs which confirms powder hydrophobicity.

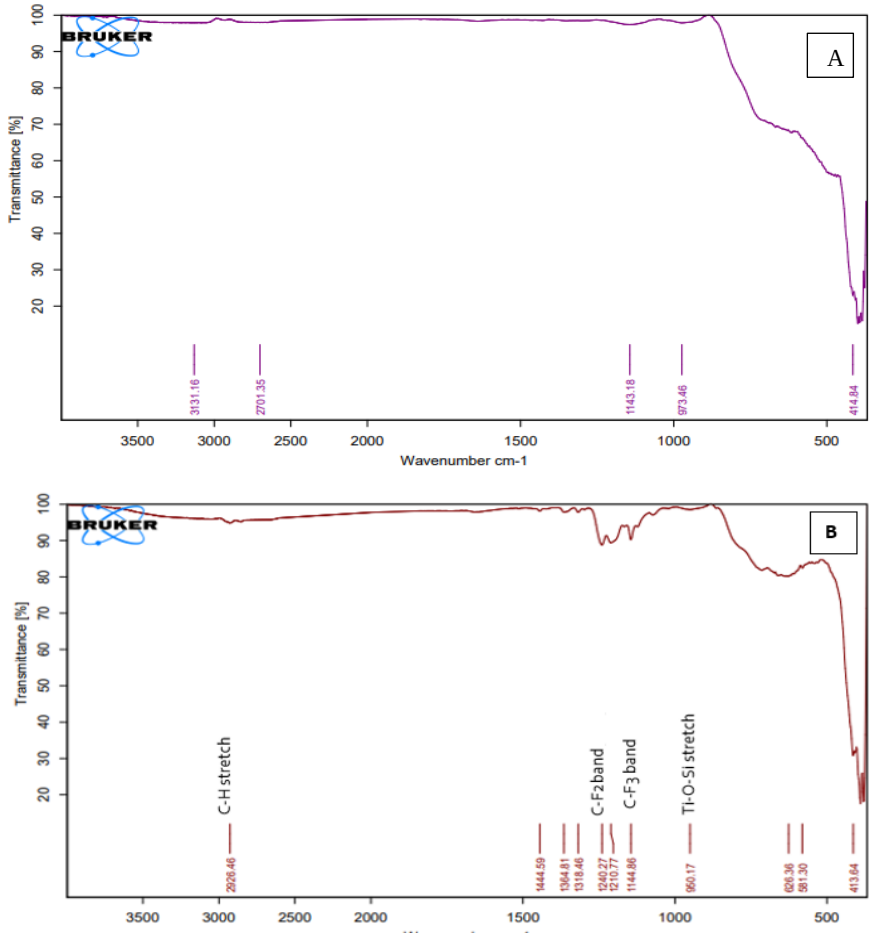

Figure 6: a) FTIR spectra of TiO_2 particles, b) FTIR spectra of FTiNPs particles

Figure 7: Digital photo of water droplet on FTiNPs particle

3.2 Membrane morphology

a. Effect of adding SiNPs in the inner layer

Membrane integrity is an important r
equirement for dual-layer hollow fibers. Strong molecular interaction may occur between the outer and inner layers. Therefore, delamination-free dual-layer hollow fibers may be achieved. Figure 8 displays the SEM cross-section and enlarged cross-section morphology of dual-layer fibers spun from the homogenous two dopes with different inner dope compositions. Overall, there is no delamination between the two polymer layers. Other than the polymer interaction, many factors also contribute to the delamination-free dual-layer structure. In the dope formulation, the inner layer dope has a lower polymer concentration than the outer layer. This results in a higher shrinkage rate in the outer layer than in the inner layer during phase inversion. As a consequence, the outer layer would tighten around the inner layer and form a seamless interface [55]. Also, since the inner layer materials TEC and FSiNPs are stretchable and the outer layer PVDF/FTiNPs is mechanically strong, this helps the easy adherence of the outer layer around the inner layer [56-57]. Figure 9 is a cross-section showing the morphology of the H/H-TBF composite membranes, at concentrations of 0.1, 0.2, and 0.4 wt. % SiNPs in the inner layer dope solution under the same spinning condition. The outer layer of the composite fiber is about to disappear when the SiNPs wt.% increased more than 0.2 wt.%. It is noticeable that the size and the shape of holes at 0.2 wt.% of SiNPs are homogeneous and perfectly rounded, which follows the distribution profile of dope velocity along the spinneret channel.

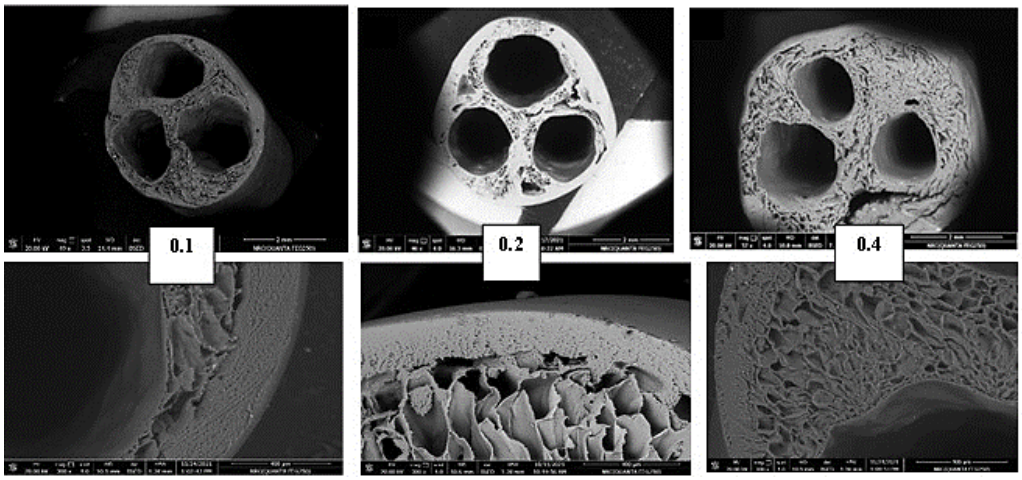

Figure 8: Cross-section and enlarged cross section morphology of TBHF Composite (dual-layer) membranes at different SiNPs wt.%

a. Effect of bore fluid flow rate

The influence of bore fluid flow rate on the membrane characteristics and performance, were investigated. Figure 9 depicts the SEM photos for H/H-TBF composite membranes with inner and outer dope flow rates of 0.63 and 1.6 ml/s respectively, at bore fluid flow rates of 0.29, 0.42 and 0.55 ml/s. The test was accomplished at the TBF blend composition of the combined outer and inner polymer coded H/H_2. As observed in Figure 10, the deformation in the TBF composite membrane occurred when the flow rate of the bore fluid is increased over 0.29 ml/s causing a remarkable deformation of TBF composite membrane. This deformation can be attributed to the uneven stress distribution on increasing the bore fluid flow rate. The high linear speed caused severe bore collapse between the three extruding streams from spinneret needles [58]. Figure 10 indicates good appearance of bores and approximate homogeneity in the bores arrangement at a bore fluid flow rate of 0.29 ml/s.

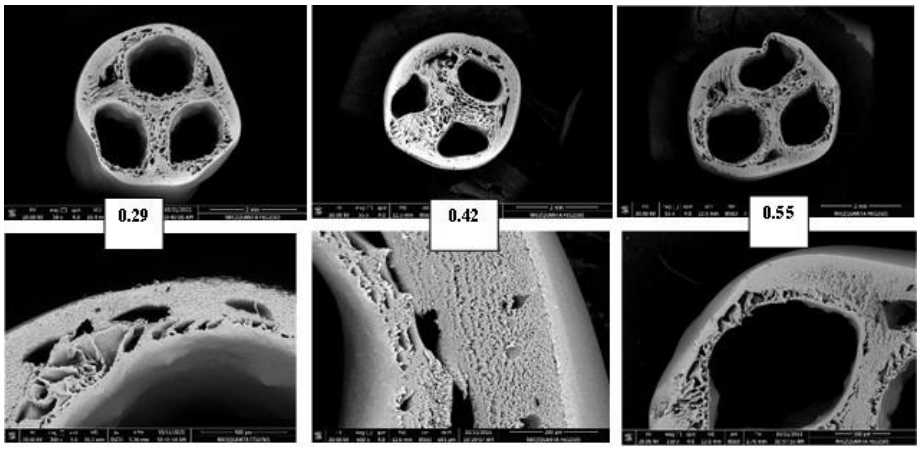

Figure 9: Cross-section morphology and magnification of TBHF Composite (dual-layer) membrane at different bore fluid flow rates (ml/s)

b. Effect of inner dope flow rate

The effect of the inner dope flow rate on the prepared TBF blend of the combined outer and inner polymer coded H/H_2 is investigated in the range of 0.29-1.6 ml/s. Figure 10 presents the SEM images of TBHF composite membranes under different flow rates of the inner dope solution (0.29, 0.63, 0.95, 1.3, 1.6 ml/s) at a fixed outer dope flow rate of 1.6 ml/s, bore fluid flow rate at 0.29 ml/s and at a 3 cm air gap distance. It is seen that the trend of approximate symmetric morphology transition of the holes and the size of the formed bore at an inner dope flow rate in the range of 0.63 and 0.95 ml/s. Increasing the inner dope solution flow rate beyond 0.95 ml/s leads to deforming the shape of the holes, and incomplete cohesion between the two-layer interfaces [58,59]. Figure 10 also indicates a decrease in the outer layer thickness as the flow rate of the inner dope increased beyond 0.95 ml/s. Accordingly, the optimum configuration was obtained at 0.95 ml/s inner dope flow rate.

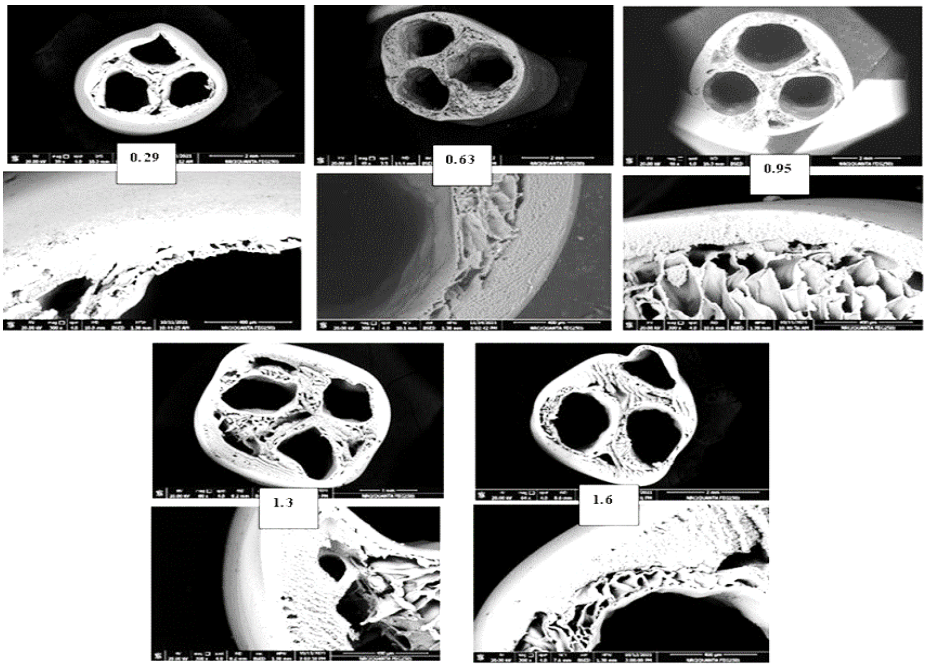

Figure 10: Cross-section of TBHF Composite (dual-layer) at different inner dope flow rates (ml/s)

c. Effect of increasing air gap distance

Figure 11 illustrates that the air gap distance of 3 cm gives a smooth shape of the fiber surface. In contrast, at an air gap of 0 cm deformation and irregular beaks are observed. When the air gap distance was increased over 3 cm, the deformation returned back. This happened due to the effect of the ambient conditions on the fibers for a relatively long time.

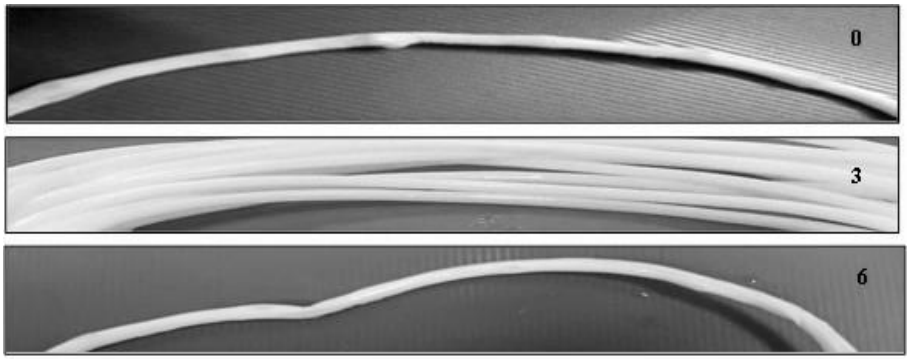

Figure 11: The external shape of TBHF Composite (dual-layer) membrane at various air gap distance (cm)

3.3 Membrane hydrophobicity

Surface hydrophobicity was measured in terms of the contact angle of the water droplet on the horizontal surface of the membrane. Surface hydrophobicity can be enhanced either by increasing surface roughness via nanoparticle blending and/or by reducing surface free energy via chemical modification [52]. The high surface hydrophobicity of the membranes is important when used in membrane distillation to avoid pore wetting and fouling. The contact angle increases when the additives are incorporated into the spinning solution. The TBHF composite membrane had the highest contact angle of 138.8° as shown in Figure 12. This is due to the positive contribution of the low surface tension fluorocarbon compound in FTiNPs particles. The cross-linked structure of the PVDF entangled the FTiNPs through attractive electrostatic forces which lead to form micro/nano structures. The MD membrane M0 had the lowest contact angle. Adding the FTiNPs to the dope solution, the hydrophobicity of the prepared membranes was enhanced as shown in figure 13.
The roughness of the resulting surface of the FTiNPs/PVDF composite surface increased. This nano-structure with multi-scale roughness was conducive to an excellent super-hydrophobic effect. Interestingly, PVDF-FTiNPs modified membranes exhibited hydrophobic characteristics as shown in Figure 12 and Figure 13.

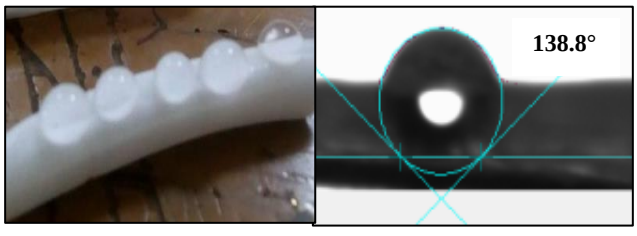

Figure 12: Water droplet on TBHF Composite membrane and its contact angle

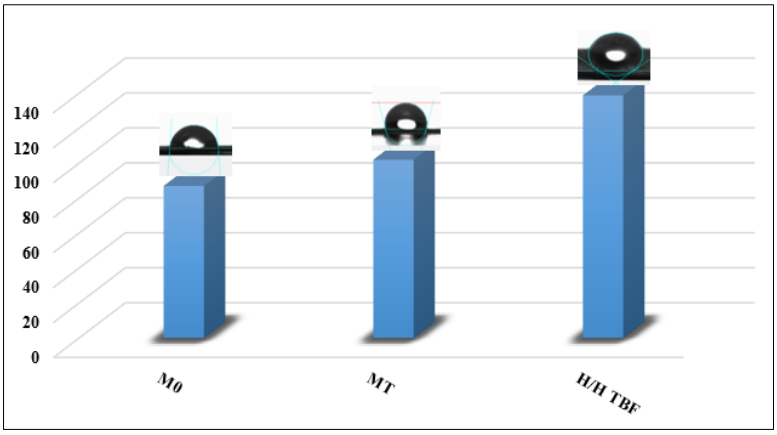

Figure 13: Contact angles for M0, MT and H/H TBF membranes

It is to be noted that the hydrophobicity of M0 could be achieved through the enhancement of surface roughness by adding FTiNPs nanoparticles [52,53]. The surface roughness of M0 and MT was further analyzed using topography images generated by the AFM instrument. Three-dimensional images shown in Figure 14 indicate that the addition of FTiNPs affected surface roughness dramatically in the case of MT flat sheet membrane.

The surface roughness (Rq) of M0 is 5.46 nm, while that of the FAS-TiO_2/ PVDF composite (MT) increased to 13.6 nm. As the CA of air is 180°, it is a hydrophobic material, indicating that trapping air contributes to strengthening surface hydrophobicity. Surface roughness plays a crucial role because air trapping in the rough surface drastically enhances surface hydrophobicity. The air is easy to be trapped in the apertures as FTiNPs/PVDF composite surface is rough enough, the AFM results further confirmed that the micro/nano structure is formed on the composite surface [60].

In the AFM images at a scan size of 100 nm, the brightest area presents the highest point of the membrane surface and the dark regions indicate valley or membrane pores. This clearly indicates that the surface morphologies of membranes were influenced by the addition of FTiNPs nanoparticles in the casting solution. It visually seems that the surface porosities of membranes prepared by adding 0.5 wt.% of FTiNPs are high compared to un-modified membranes. The pore sizes of the membranes decreased because of the filling of the membrane pores by entrapping inorganic n-particles in the polymeric matrix. This results in improved membrane porosity and an increase in the number of small pores with micro and nanostructures as shown in figure 15 [61].

3.4 Mechanical properties of TBHFC membrane

The newly developed dual-layer TBHF composite membrane has a much higher maximum tensile strain compared to other PVDF fibers [38,48]. Compared to tri-bore and dual-layered PVDF fibers, the maximum strain increases to about 200% and 500%, respectively as shown in Figure 16. Although the multi-bore PVDF fibers have better mechanical properties than single-bore fibers, they are still mechanically weaker than the dual-layer TBHFC fibers. Incorporating SiNPs and TEC in the inner layer dope, reinforces the dual-layer hollow fiber thus enhancing the mechanical properties of the inner support layer. The newly developed multi-bore dual-layer membranes would thus be suitable for MD applications, especially VMD because it has stringent requirements on membrane mechanical strength.

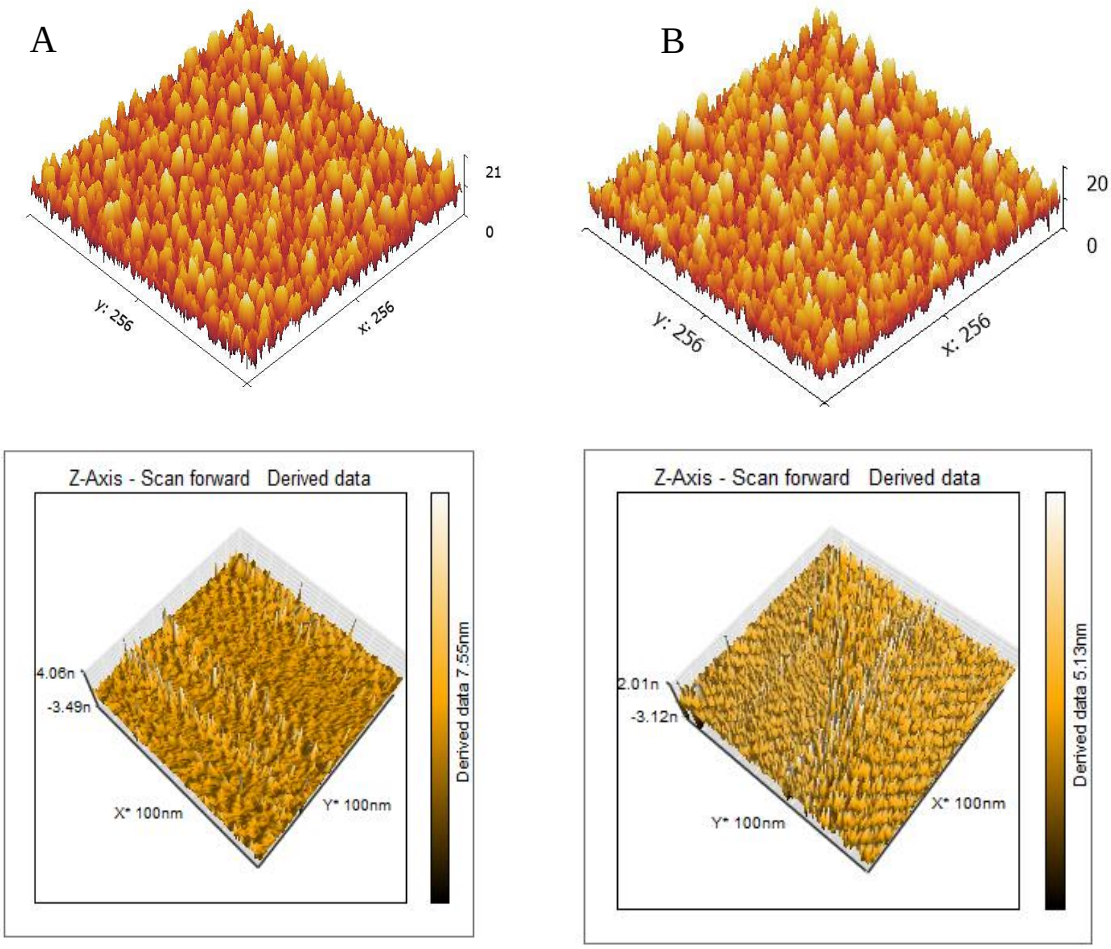

Figure 14. Three -dimension AFM pictures depicting the change of outer surface morphology for a) M0, b) MT

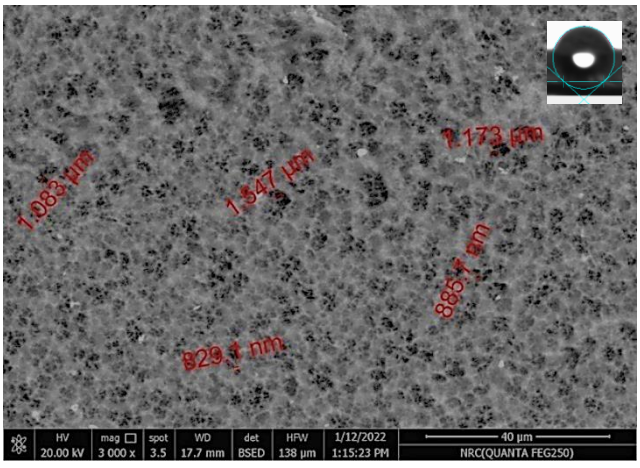

Figure 15: SEM images of top surface magnification 3000x for H/H_2- TBF6 membrane

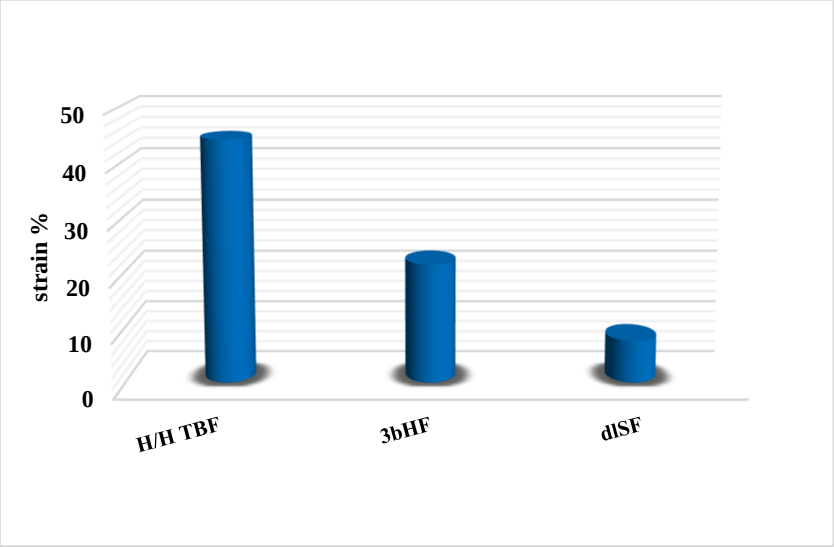

Figure 16: Tensile strain at break of different investigated membranes

3.5 Membranes performance in VMD unit

The performance of the fabricated H/H TBF (TBF-6), M0, and MT membranes in VMD desalination is conducted for 30 min. The inlet temperature of the feed solution is increased to 65°C. The permeation flux and salt rejection are presented in Table 3, which shows that the permeation flux is slightly increased when MT is used. A noticeable increase when using TBF-6 instead of MT flat sheet membrane is evident. The permeation flux reached 27.3 l/m^2.h and 19.4 l/m^2.h for the hydrophobic/hydrophilic TBF (TBF6) and the flat sheet membrane (MT) prepared from the same outer layer dope composition, respectively. TBF membrane also gave an acceptable salt rejection, 97.8% of the salt was not allowed to penetrate through the membrane.

Table 3 membranes performance in VMD unit

Membrane code	Permeate flux (lit/m^2.h)	Salt rejection %
M0	15.5	98.9
MT	19.4	98.8
H/H2-TBF6	27.3	97.8

4. Conclusions

A dual-layer tri-bore hollow fiber (H/H -TBF) membranes with super hydrophobic outer layer were prepared by a dry-wet jet spinning process using polyvinylidene, superhydrophobic TiO_2 nanoparticles in the outer layer, and SiO_2 in the inner layer. The thin top layer was optimized by adding 0.5 wt% of FTiNPs in the dope solution. The contact angle increased to 138.8°. Moreover, the membrane became more elastic and stretchable due to adding 0.2 wt.% SiO_2 nanoparticles and TEC into the inner layer. The prepared membrane showed a comparable strain at a break of 44.51% with the dual-layered single bore hollow fiber PVDF membrane having a strain of 7.9%. Combining the outer layer with micro and nanostructures with a porous support layer,

membranes can be used for a stable membrane distillation process with high flux. The prepared H/H-TBF membrane showed a higher flux than the dual-layered flat sheet membrane. Due to its enhanced properties such as significantly higher hydrophobicity, strain%, and porosity, the prepared H/H -TBF membrane exhibited higher flux (27.3 lm^{-2} h^{-1}) compared to the flat sheet PVDF membrane (15.5 lm^{-2} h^{-1}) while still maintaining a stable operation.

Acknowledgements

The authors acknowledge the financial support of the [Academy of Scientific Research and Technology (ASRT)] under Grant [number 2/2019/ASRT-Nexus] Project ID: 4365

Disclosure statement

No potential conflict of interest was reported by the author(s)

References

[1] Rifaat Abdel Wahaab, Waleed H. Elsayed, Mahmoud S. Ibrahiem, Amany F. Hasballah, Application of Water Safety Plans to Improve Desalination Water Supply at Matrouh Governorate, Egypt, Egypt. J. Chem. Vol. 64, No. 11 pp. 6749 – 6759, 2021.

[2] Al Hathal Al-Anezi, A. O. Sharif, M. I. Sanduk, and A. R. Khan, Potential of membrane distillation—a comprehensive review, International Journal of Water, vol. 7, no. 4, pp. 317–346, 2013.

[3] L. M. Camacho, L. Dume e, J. hang et al., Advances in membrane distillation for water desalination and purification applications, Water, vol. 5, no. 1, pp. 94–196, 2013.

[4] P. Wang and T.-S. Chung, ―Recent advances in membrane distillation processes: membrane development, configuration design and application exploring, Journal of Membrane Science, vol. 474, pp. 39–56, 2015. DOI: http://dx.doi.org/10.1016/j.memsci.2014.09.016

[5] M. S. El-Bourawi, Ding, R. Ma, and M. Khayet, A framework for better understanding membrane distillation separation process, Journal of Membrane Science, vol. 285, no. 1-2, pp. 4–29, 2006.

[6] A. A. Alanezi and A.O. Sharif, ―Membrane distillation: an attractive alternative, Arab Water World, vol. 36, no. 5, pp. 1– 77, 2012.

[7] M. A. Eltawil, Z. Zhengming, and L. Yuan, ―A review of renewable energy technologies integrated with desalination systems, Renewable and Sustainable Energy Reviews, vol. 13, no. 9, pp. 2245–2262, 2009.

[8] Mohammed Karama Alsebaeai, Abdul Latif Ahmad, Membrane distillation: Progress in the improvement of dedicated membranes for enhanced hydrophobicity and desalination performance, Journal of Industrial and Engineering Chemistry 86 (2020) 13–34

[9] L. Eykens, K. De Sitter, C. Dotremont, L. Pinoy, B. Van der Bruggen, Membrane synthesis for membrane distillation: A review, Separation and Purification Technology (2017), doi: http://dx.doi.org/10.1016/ j. seppur.2017.03.035

[10] Guo-dong Kangn, Yi-ming Caonn, Application and modification of poly (vinylidene fluoride) (PVDF) membranes – A review, Journal of Membrane Science 463 (2014) 145–165146.

[11] Fu Liu1, N. Awanis Hashim, Yutie Liu, M.R. Moghareh Abed, K. Li, Progress in the production and modification of PVDF membranes, Journal of Membrane Science 375 (2011) 1–27

[12] L. Shi, R. Wang, Y. Cao, D.T. Liang, J.H. Tay, Effect of additives on the fabrication of poly (vinylidene fluoride-co-hexafluropropylene) (PVDF-HFP) asymmetric microporous hollow fiber membranes, J. Membr. Sci. 315 (2008) 195-204

[13] M.M. Teoh, T.S. Chung, Membrane distillation with hydrophobic macrovoid-free PVDF–PTFE hollow fiber membranes, Sep. Purif. Technol. 66 (2009) 229–236.

[14] M.C. García-Payo, M. Essalhi, M. Khayet, Preparation and characterization of PVDF– HFP copolymer hollow fiber membranes for membrane distillation, Desalination, 245 (2009) 469-473.

[15] D.Y. Hou, J. Wang, D. Qu, Fabrication and characterization of hydrophobic PVDF hollow fiber membranes for desalination through direct contact membrane distillation, Sep. Purif. Technol. 69 (2009) 78–86.

[16] K.Y. Wang, T.S. Chung, M. Gryta, Hydrophobic PVDF hollow fiber membranes with narrow pore size distribution and ultra-thin skin for the fresh water production through membrane distillation, Chem. Eng. Sci. 63 (2008) 2587–2594.

[17] X. Yang, R. Wang, L. Shi, A.G. Fane, M. Debowski, Performance improvement of PVDF hollow fiber-based membrane distillation process, J. Membr. Sci. 369 (2011) 437– 447.

[18] N. Peng, N. Widjojo, P. Sukitpaneenit, M.M. Teoh, G.G. Lipscomb, T.S. Chung, J.Y. Lai, Evolution of polymeric hollow fibers as sustainable technologies: past, present and future, Prog. Polym. Sci. 37 (2012) 1401–1424.

[19] Y. Tang, N. Li, A. Liu, S. Ding, C. Yi, H. Liu, Effect of spinning conditions on the structure and performance of hydrophobic PVDF hollow fiber membranes for membrane distillation, Desalination 287 (2012) 326–339.

[20] Pengfei Zhang, Wenyi Liu, Saeid Rajabzadeh, Yuandong Jia, Qin Shen ,Chuanjie Fang ,Noriaki Kato ,Hideto Matsuyama, Modification of PVDF hollow fiber membrane by co-deposition of PDA/MPC-co-AEMA for membrane distillation

application with anti-fouling and anti-scaling properties, Journal of Membrane Science, Volume 636, 15 October 2021, 119596
[21] Lijo Francis, Noreddine Ghaffour, Ahmad S. Al-Saadi, Gary Amy, Performance of Different Hollow Fiber Membranes for Seawater Desalination Using Membrane Distillation, Desalination and Water
Treatment, 55(10), 2786–2791. doi:10.1080/19443994.2014.946723
[22] M.M. Teoh, T.S. Chung, Membrane distillation with hydrophobic macrovoid free PVDF-PTFE hollow fiber membranes, Sep. Purif. Technol. 66 (2009)229–236.
[23] M.F. Shaaban, M.A. El-Khateeb and M.A. Saad, Water Desalination Using Cellulosic Nano-filtration Membrane Composed of Nano-scale Polytetraflouroethylene, Egypt. J. Chem. (2019). Vol. 62, No.1 pp.15 - 20.
[24] Fida Tibi, Seong-Jik Park and Jeonghwan Kim, Improvement of Membrane Distillation Using PVDF Membrane Incorporated with TiO_2 Modified by Silane and Optimization of Fabricating Conditions, Membranes 2021, 11, 95.
[25] N. Hamzah, C.P. Leo, Membrane distillation of saline with phenolic compound using superhydrophobic PVDF membrane incorporated with TiO_2 nanoparticles: Separation, fouling and self-cleaning evaluation, Desalination 418 (2017) 79–88
[26] Elsayed M. Elnaggar , Mohamed E.A. Ali, Mostafa M. Abo-Elfadl, Ehab S. Gad , Salah F. Abdellah, Amr A. Sammak, Gamal M. El-kady, Performance of Nanocomposite Polysulfone-Polyaniline Substrates for Enhanced Thin Film Membranes, Egypt. J. Chem. (2022). Vol. 65, No.10 pp.3 -3
[27] Z. Ma, Y. Hong, L. Ma, M. Su, Superhydrophobic membranes with ordered arrays of nanospiked microchannels for water desalination, Langmuir 25 (2009) 5446–5450
[28] Lihua Zhaoa , Chunrui Wu , Xiaolong Lu , Derrick Ng, Yen Bach Truong, Zongli Xie,, Activated carbon enhanced hydrophobic/hydrophilic dual-layer nanofiber composite membranes for high-performance direct contact membrane distillation, Desalination 446 (2018) 59–69
[29] : B. Xie, G. Xu, Y. Jia, L. Gu, Q. Wang, N. Mushtaq, B. Cheng, Y. Hu, Engineering carbon nanotubes enhanced hydrophobic membranes with high performance in membrane distillation by spray coating, Journal of Membrane Science (2021), doi: https://doi.org/10.1016/ j.memsci.2020.118978.
[30] Lihua Zhao, Chunrui Wu, Xiaolong Lu, Derrick Ng, Yen Bach Truong, Zongli Xie , Activated carbon enhanced hydrophobic/hydrophilic dual-layer nanofiber composite membranes for high-performance direct contact membrane distillation, Desalination 446 (2018) 59–69.
[31] Jiaming Zhu, Lanying Jiang, Takeshi Matsuura, New insights into fabrication of hydrophobic/hydrophilic composite hollow fibers for direct contact membrane distillation, Chemical Engineering Science 137 (2015) 79–9080.
[32] M. Su, M.M. Teoh, K.Y. Wang, J. Su, T.S. Chung, Effect of inner-layer thermal conductivity on flux enhancement of dual-layer hollow fiber membranes in direct contact membrane distillation, J. Membr. Sci. 364 (2010) 278–289.
[33] Felinia Edwie, May May Teoh, Tai-Shung Chung, Effects of additives on dual-layer hydrophobic–hydrophilic PVDF hollow fiber membranes for membrane distillation and continuous performance, Chemical Engineering Science 68 (2012) 567–57.
[34] Jun Li, Long-Fei Ren, Jiahui Shao, Yonghui Tu, Zhongbao Ma, Yuanxin Lin, Yiliang He, Fabrication of triple layer composite membrane and its application in membrane distillation (MD): Effect of hydrophobic-hydrophilic membrane structure on MD performance, Separation and Purification Technology 234 (2020) 116087
[35] Sina Bonyadi, Tai Shung Chung, Flux enhancement in membrane distillation by fabrication of dual layer hydrophilic–hydrophobic hollow fiber membranes, journal of Membrane Science 306 (2007) 134–146.
[36] Peng Wang, May May Teoh, Tai-Shung Chung, Morphological architecture of dual-layer hollow fiber for membrane distillation with higher desalination performance, water research 45 (2011) 5489 e5500.
[37] Na Peng, May MayTeoh, Tai-Shung Chung, Ley Ling Koo, Novel rectangular membranes with multiple hollow holes for ultrafiltration, Journal of Membrane Science 372 (2011) 20–28
[38] Elham El-Zanati, Maaly Khedr, Eman Farag and Esraa Taha, Fabrication of Tri-bore Hollow Fiber (TBF) Membrane Module for Vacuum Membrane Distillation, Wat.Ener.Food.Env.J 1, No. 2, 25-35(2020).
[39] Elham M. El-Zanati, Eman Farg, Esraa Taha, Ayman El-Gendi and Heba Abdallah, Preparation and characterization of different geometrical shapes of multi-bore hollow fiber membranes and application in vacuum membrane distillation, Journal of Analytical Science and Technology, https://doi.org/10.1186/s40543-020-00244-4, (2020) 11:47
[40] P. Wang, T.-S. Chung, design and fabrication of lotus-root -like multi -bore hollow fiber membrane for direct contact membrane distillation,

Journal of Membrane Science 421–422 (2012) 361–374362.
[41] Peng Wang, and Tai-Shung Chung, A New-Generation Asymmetric Multi-Bore Hollow Fiber Membrane for Sustainable Water Production via Vacuum Membrane Distillation, Environ. Sci. Technol.DOI: 10.1021/es400356z, Publication Date (Web): 10 May 2013.
[42] Peng Wang, Tai-Shung Chung, Design and fabrication of lotus-root-like multi-bore hollow fiber membrane for direct contact membrane distillation, Journal of Membrane Science 421–422 (2012) 361–374.
[43] Dan Hua, Yee Kang Ong, Peng Wang, Tai-Shung Chung. Thin-film composite tri-bore hollow fiber (TFCTbHF) membranes for isopropanol dehydration by pervaporation, Journal of Membrane Science 471(2014)155–167.
[44] Elham ElZanati, Novel Membranes with Multiple Hollow Holes (MMHH) for Reaction Catalysis to produce biofuel, ID: 9185, 2016.
[45] Amir Razmjou, Ellen Arifin, Guangxi Dong, Jaleh Mansouri, Vicki Chen, Superhydrophobic modification of TiO_2 nanocomposite PVDF membranes for applications in membrane distillation, Journal of Membrane Science 415–416 (2012) 850–863
[46] Wei Zhang, Ying Li, Jun Liu, Baoan Li, Shichang Wang, Fabrication of hierarchical poly (vinylidene fluoride) micro/nano-composite membrane with anti-fouling property for membrane distillation, Journal of Membrane Science 535 (2017) 258–267.
[47] Jafar Zahirifar , Javad Karimi-Sabet , Seyed Mohammad Ali Moosavian , Alireza Hadi, Parisa Khadiv-Parsi, Fabrication of a novel octadecylamine functionalized graphene oxide/PVDF dual-layer flat sheet membrane for desalination via air gap membrane distillation, Desalination 428 (2018) 227–239.
[48] Jian Zuo, Tai-Shung Chung, Gregory S. O'Brien, Walter Kosar, Hydrophobic/hydrophilic PVDF/Ultem® dual-layer hollow fiber membranes with enhanced mechanical properties for vacuum membrane distillation, Journal of Membrane Science 523 (2017) 103–110.
[49] Paola Bernardo, Sabrina Pret, Gabriele Clarizi, Franco Tasselli, Effect of external fluid and inline crosslinking on the performance of polyimide hollow fibres prepared by using a triple–orifice spinneret, Journal of Membrane Science 570–571 (2019) 410–417.
[50] Minglue Su, May May Teoh, Kai Yu Wang, Jincai Su, Tai-Shung Chung, Effect of inner-layer thermal conductivity on flux enhancement of dual-layer hollow fiber membranes in direct contact membrane distillation, Journal of Membrane Science 364 (2010) 278–289.
[51] Y. Qing et al. Superhydrophobic TiO_2/polyvinylidene fluoride composite surface with reversible wettability switching and corrosion resistance, Chemical Engineering Journal 290 (2016) 37–4
[52] N. Hamzah, C.P. Leo, Membrane distillation of saline with phenolic compound using superhydrophobic PVDF membrane incorporated with TiO_2 nanoparticles: Separation, fouling and self-cleaning evaluation, Desalination 418 (2017) 79–88
[53] Eyad M.Hamad, SamerAl-Gharabli, JoannaKujaw, Tunable hydrophobicity and roughness on PVDF surface by grafting to mode – Approach to enhance membrane performance in membrane distillation process, Separation and Purification Technology, Volume 291, 15 June 2022, 120935.
[54] Eui-Jong Lee, Alicia Kyoungjin An, Pejman Hadi, Sangho Lee, Yun Chul Woo, Ho Kyong Shon, Advanced multi-nozzle electrospun functionalized titanium dioxide/ polyvinylidene fluoride-co-hexafluoropropylene (TiO_2/PVDF-HFP) composite membranes for direct contact membrane distillation, Journal of Membrane Science 524 (2017) 712–72.
[55] Dongfei Li, Tai-Shung Chung, Rong Wang, Morphological aspects and structure control of dual-layer asymmetric hollow fiber membranes formed by a simultaneous co-extrusion approach, Journal of Membrane Science , Volume 243, Issues 1–2, 1 November 2004, Pages 155-175
[56] Georgy Kagramanov, Vladimir Gurkin, and Elena Farnosova, Physical and Mechanical Properties of Hollow Fiber Membranes and Technological Parameters of the Gas Separation Process, Membranes (Basel). 2021 Aug; 11(8): 583.
[57] Hazlini Dzinun, Mohd Hafiz Dzarfan Othman, A.F.Ismail, Mohd Hafiz Puteh, Mukhlis A.Rahman, Juhana Jaaf, Morphological study of co-extruded dual-layer hollow fiber membranes incorporated with different TiO_2 loadings, Journal of Membrane Science Volume 479, 1 April 2015, Pages 123-131
[58] K.Y. Wang, T. Matsuura, T.S. Chung, W.F. Guo, The effects of flow angle and shear rate within the spinneret on the separation performance of poly(ethersulfone) (PES) ultrafiltration hollow fiber membranes, J. Membr. Sci. 240 (2004).
[59] S. Bonyadi, T.S. Chung, W.B. Krantz, Investigation of corrugation phenomenon in the inner contour of hollow fibers during the non-solvent induced phase separation, process, J. Membr. Sci. 299 (2007) 200.

[60] Fadhela M Hussein; Yousif kadhim Al-Haidarie; Ramzie Rasheed Alani; ALI AL-MOKARAM, synthesis and Photocatalytic Activity of TiO_2-coupled SnO_2 Nanoparticles Prepared by Sol–Gel Technique, Egypt. J. Chem. (2022). Vol. 65, No.10 pp.1 -5.
[61] Wei Zhang, Ying Li, Jun Liu, Baoan Li, Shichang Wang, Fabrication of hierarchical poly (vinylidene fluoride) micro/nano-composite membrane with anti-fouling property for membrane distillation, Journal of Membrane Science 535 (2017) 258–26